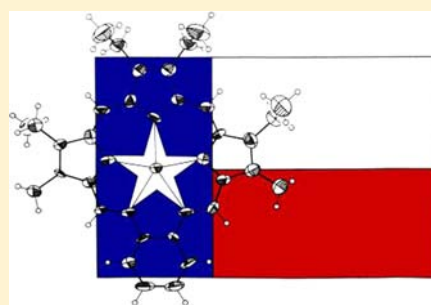


## Recent Developments in Texaphyrin Chemistry and Drug Discovery

Christian Preihs,<sup>†</sup> Jonathan F. Arambula,<sup>†,‡</sup> Darren Magda,<sup>§</sup> Heeyeong Jeong,<sup>||</sup> Dongwon Yoo,<sup>||</sup> Jinwoo Cheon,<sup>||</sup> Zahid H. Siddik,<sup>‡</sup> and Jonathan L. Sessler<sup>\*,†,||</sup><sup>†</sup>Department of Chemistry and Biochemistry, University of Texas, 1 University Station, A5300, Austin, Texas 78712-0165, United States<sup>§</sup>Lumiphore, Inc., 4677 Meade Street, Richmond, California 94804, United States<sup>||</sup>Department of Chemistry, Yonsei University, Seoul 120-749, Korea<sup>‡</sup>Department of Experimental Therapeutics, UT M. D. Anderson Cancer Center, 1515 Holcombe Boulevard, Unit 1950, Houston, Texas 77030, United States

**ABSTRACT:** Texaphyrins are pentaaza expanded porphyrins with the ability to form stable complexes with a variety of metal cations, particularly those of the lanthanide series. In biological milieus, texaphyrins act as redox mediators and mediate the production of reactive oxygen species (ROS). In this review, newer studies involving texaphyrin complexes targeting several different applications in anticancer therapy are described. In particular, the preparation of bismuth and lead texaphyrin complexes as potential  $\alpha$ -core emitters for radiotherapy is detailed, as are gadolinium texaphyrin functionalized magnetic nanoparticles with features that make them of interest as dual-mode magnetic resonance imaging contrast agents and as constructs with anticancer activity mediated through ROS-induced sensitization and concurrent hyperthermia. Also discussed are gadolinium texaphyrin complexes as possible carrier systems for the targeted delivery of platinum payloads.



The combined use of chemotherapy and radiation therapy has led to clinical breakthroughs in the controlled treatment and cure of several cancerous diseases. Today, the three main types of radiation therapy are classified as external beam radiation therapy (EBRT or more commonly X-ray therapy, XRT), brachytherapy (sealed source radiation therapy), and systematic radioisotope therapy (unsealed source radiotherapy). However, the search for efficient radiation sensitizers, i.e., compounds that actively support radiation therapy through different mechanisms, remains a critical, albeit elusive, goal in anticancer therapy. Active, or so-called sensitized, radiation therapy could prove particularly beneficial in the treatment of solid tumors. Solid tumors usually outgrow their blood supply, causing a low-oxygen state known as hypoxia. As revealed by modern detection techniques, these hypoxic regions are often characterized by reduced XRT efficiencies. In the absence of oxygen, DNA is repaired more efficiently. In contrast, oxygenated tissues are generally 2 to 3 times more sensitive toward radiation. From an operational perspective, hypoxic cells are difficult to destroy completely using XRT alone.<sup>1,2</sup> Applying radiation sensitizers could allow modulation of the radiation response and lead to an improvement in local tumor control. Here, the idea is to administer radiosensitizers that would enhance or support the effects of radiation at cancerous sites, reduce cytotoxic side effects for normal tissues, or both.

Oxygen-derived species, such as superoxide, singlet oxygen, hydroxyl radicals, and hydrogen peroxide, are prominent cytotoxic substances and have been implicated in the etiology

of a wide array of human diseases, including cancer. When administered in a cancer-selective manner, drugs that are able to produce reactive oxygen species (ROS) can give rise to manifest benefits. Several classes of anticancer drugs, such as quinone-based agents, have been studied as a means to promote the generation of ROS at tumor sites.<sup>3</sup> The mechanism is believed to involve a redox cycling process that relies, in part, on chemical reduction *in vivo* by biological reductants, such as nicotinamide adenine dinucleotide phosphate (NADPH); reoxidation with oxygen produces ROS that can *inter alia* damage DNA.

Many strategies to enhance the efficacy of radiation therapy involve diminishing the activity of natural ROS defense mechanisms. Often enzymes, such as superoxide dismutase, glutathione peroxidase, and catalase, are involved. Many other endogenous species, including glutathione (GSH), thioredoxin/thioredoxin reductase (TRXR), ascorbate (vitamin C), and  $\alpha$ -tocopherol (vitamin E), are also able to serve as ROS scavengers. Agents that either compromise these defense mechanisms or are able to produce actively enhanced levels of ROS are thus attractive because they could lead to more efficient anticancer treatments.

**Texaphyrin, a Redox-Active Expanded Porphyrin.** Several classes of Food and Drug Administration (FDA)-approved anticancer drugs, including quinone-based agents, are

**Special Issue:** Metals in Medicine and Health

**Received:** January 29, 2013

**Published:** April 4, 2013

believed to exhibit radiation-sensitizing effects as a result of producing ROS, such as superoxide and hydrogen peroxide. These latter entities are able to damage DNA and promote cell death. Texaphyrins are experimental drugs that are known to localize to cancerous lesions and to produce ROS. This is discussed further below.

Texaphyrins are pentaaza Schiff base macrocycles with a strong, but “expanded”, similarity to traditional porphyrins.<sup>4–6</sup> They also bear resemblance to the five-pointed star in the state flag of Texas, a feature that accounts for their name. From a chemical perspective, texaphyrins are characterized by the presence of an inner coordination core that is roughly 20% larger than that present in porphyrins. The formal charge on the deprotonated texaphyrin ligand is 1–, compared to 2– for a porphyrin. To date, the texaphyrins have been demonstrated to form stable 1:1 complexes with a wide variety of metal cations, particularly with those of the trivalent lanthanide series (cf. Figure 2).<sup>4,7,8</sup>

One particular functionalized gadolinium(III) texaphyrin, motexafin gadolinium (**1**; Figure 1) has been studied in detail

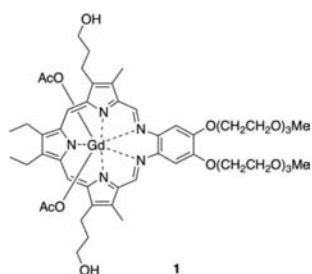


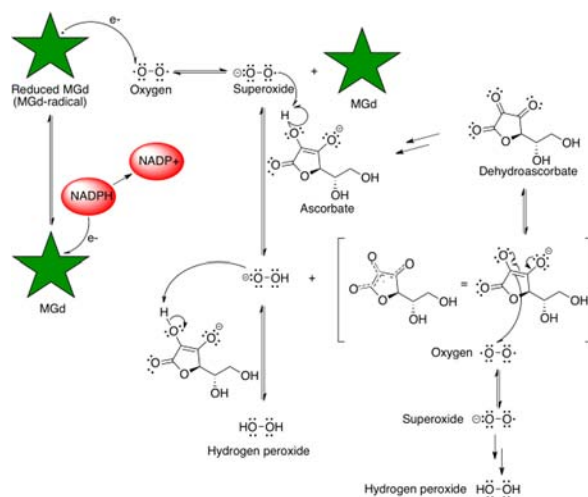
Figure 1. Structure of **1**.

H																	He
Li	Be											B	C	N	O	F	Ne
Na	Mg											Al	Si	P	S	Cl	Ar
K	Ca	Sc	Ti	V	Cr	Mn	Fe	Co	Ni	Cu	Zn	Ga	Ge	As	Se	Br	Kr
Rb	Sr	Y	Zr	Nb	Mo	Tc	Ru	Rh	Pd	Ag	Cd	In	Sn	Sb	Te	I	Xe
Cs	Ba	La	Hf	Ta	W	Re	Os	Ir	Pt	Au	Hg	Tl	Pb	Bi	Po	At	Rd
Fr	Ra	Ac															
Lanthanides		Ce	Pr	Nd	Pm	Sm	Eu	Gd	Tb	Dy	Ho	Er	Tm	Yb	Lu		
Actinides		Th	Pa	U	Np	Pu	Am	Cm	Bk	Cf	Es	Fm	Md	No	Lr		

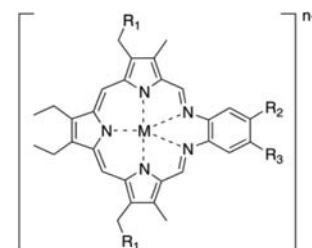
Figure 2. Known stable texaphyrin complexes with all metals shown in green.

by the Sessler group and was developed for clinical study under the aegis of Pharmacyclics, Inc.<sup>3,9</sup> In a series of physical chemical and mechanistic studies, it was shown that the gadolinium species **1** is easy to reduce in comparison to, e.g., typical porphyrins, and can act as a redox mediator producing ROS in the presence of suitable reductants and molecular oxygen (Scheme 1). In the intracellular environment, it has been proposed that complex **1** accepts an electron from, and catalyzes the oxidation of, various reducing metabolites, such as ascorbate, reduced NADPH, TRXR, GSH, and dihydroliipoate. This electron-transfer event leads to the formation of a reduced texaphyrin radical, which then reacts with oxygen to produce superoxide in a rapid equilibrium process, which, in turn, regenerates compound **1**. In vitro, and presumably in vivo, this superoxide is converted quickly into hydrogen peroxide,<sup>10</sup> a species that is known to be a potent apoptosis trigger.

### Scheme 1. Mechanistic Representation of How **1** Is Thought To Act as a Redox Mediator



In an effort to determine whether the centrally coordinated metal cation plays a role in regulating the ability of texaphyrins to function as oxidation catalysts for ascorbate, several transition-metal complexes were prepared and characterized. A summary of representative stable texaphyrin species, including various lanthanide complexes, is given in Figure 3.<sup>4,11–17</sup>



- $R_1 = R_2 = R_3 = \text{H}$ ,  $n = 1$  for  $M = \text{Cd, Zn, Mn, Hg}$ ;  $n = 2$  for  $M = \text{Nd, Sm, Eu}$
- $R_1 = \text{H}$ ,  $R_2 = R_3 = \text{Me}$ ,  $n = 2$  for  $M = \text{Sm, Eu, Gd}$
- $R_1 = \text{H}$ ,  $R_2 = R_3 = \text{OMe}$ ,  $n = 2$  for  $M = \text{Ce, Pr, Nd, Sm - Lu}$
- $R_1 = (\text{CH}_2)_2\text{OH}$ ,  $R_2 = R_3 = \text{O}(\text{CH}_2)_3\text{OH}$ ,  $n = 2$  for  $M = \text{La, Ce, Pr, Nd, Sm - Lu}$
- $R_1 = (\text{CH}_2)_2\text{OH}$ ,  $R_2 = R_3 = \text{O}(\text{CH}_2\text{CH}_2\text{O})_3\text{Me}$ ,  $n = 2$  for  $M = \text{Mn, Co}$ ;  $n = 3$  for  $\text{Fe}$

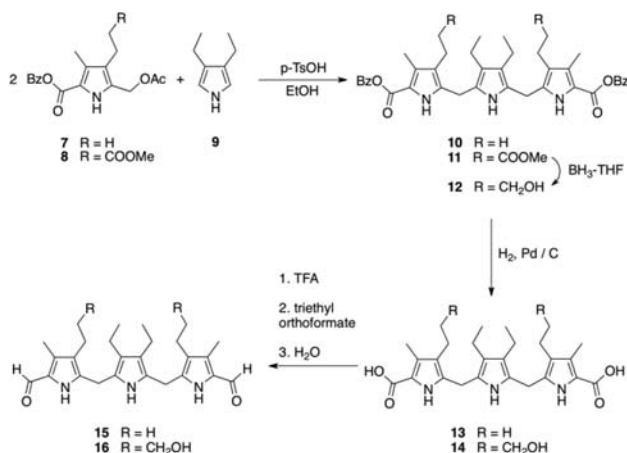
Figure 3. Summary of representative stable texaphyrin complexes.<sup>4,11–17</sup>

The role of the chelated metal center was found to be substantial. While the manganese(II) complex of texaphyrin ligand **6** displayed an initial rate that was approximately 3 times slower than that of **1** under identical experimental conditions ( $V_0 = 3.0$  vs  $8.7 \mu\text{M min}^{-1}$ , respectively), the cobalt(II) and iron(III) (as the  $\mu$ -oxo dimer) complexes of texaphyrin ligand **6** gave initial rate values ( $V_0 = 23.8$  and  $30.6 \mu\text{M}$ , respectively) that were substantially larger.<sup>18</sup> This proved true in spite of the fact that these species are *harder* to reduce than **1** [ $E_{1/2} = -571$  for **6** as the cobalt(II) complex vs  $-294$  for **1** vs  $\text{Ag/AgCl}$  in dimethyl sulfoxide].<sup>19</sup> In this instance, it is thought that the redox-active metal centers participate in ascorbate decomposition. Unfortunately, the cobalt(II) and iron(III) complexes of **6** were considered too lipophilic to be attractive in terms of further drug development, at least for the XRT sensitization indications for which **1** was being tested.

**Synthesis of Texaphyrins, Physical Properties, and Magnetic Resonance Imaging (MRI) Activity.** The synthesis of the first texaphyrins benefited from an efficient

synthesis of a symmetric tripyrrane dialdehyde key precursor. This intermediate, shown as compounds **15** and **16** in Scheme 2, was obtained via the condensation of two pyrrole subunits, **7**

### Scheme 2. Synthesis of the Texaphyrin Key Precursors **15** and **16**

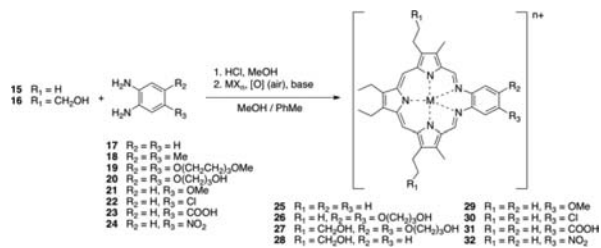


or **8** (obtained via Paal–Knorr reactions) and **9** (prepared using the Barton–Zard procedure), respectively, followed by further functional group elaboration. These latter reactions included ester deprotection, decarboxylation, and formylation. Reduction of the side-chain terminal ester to the corresponding alcohol was also carried out during the sequence of steps leading to **16**.

The nonaromatic form of the texaphyrin ligand is synthesized by a hydrogen chloride catalyzed 1:1 Schiff base condensation between a tripyrrane dialdehyde, such as **15** or **16**, with an appropriately derivatized *o*-phenylenediamine under conditions of high dilution. This procedure is similar to the one employed by Mertes et al. for formation of the so-called “accordion” macrocycle.<sup>20,21</sup>

Oxidation of the nonaromatic texaphyrin ligand in the presence of an appropriate metal salt, molecular oxygen (air), and an organic base (e.g., triethylamine) generally affords the aromatic texaphyrin macrocycle as its metal complex in good yield (Scheme 3). The metal cation is thought to stabilize the

### Scheme 3. General Synthesis of Texaphyrin



macrocycle as a result of a presumed thermodynamic template effect.<sup>22</sup> Thus, once formed these metal complexes are extremely stable, except under acidic conditions, which readily lead to hydrolysis of the macrocycle.<sup>23</sup>

The UV–visible spectrum of compound **1** is dominated by two absorption bands. The higher-energy Soret-like band at 474 nm is analogous to the ~400 nm band of porphyrins and is characteristic of the absorption bands seen for other vividly pigmented porphyrin moieties. The Soret-like band is flanked

by N- and Q-like bands at higher and lower energies, respectively, with the lowest-energy Q band for **1** being seen at 740 nm (cf. Figure 4).

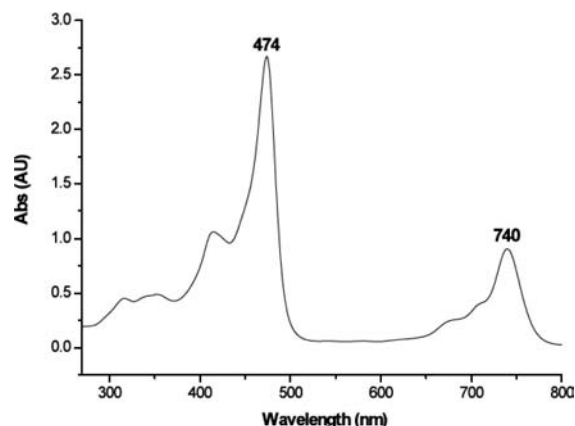


Figure 4. UV–visible spectrum of **1**, 25 μM in methanol.

Interestingly, there is a steady shift in the Q-like band from red to blue ( $\Delta = 15$  nm) as the lanthanide(III) cation under study progresses from lanthanum to lutetium.<sup>24</sup> This shift in the Q-like bands appears to follow contraction of the metal cations in the lanthanide series. A plot of the wavelength (in nanometers) of the Q-like band versus the ionic radius of the lanthanide(III) ion gives a linear relationship.<sup>24</sup>

Another spectral feature of certain metalated texaphyrins, especially those containing diamagnetic cations, is their ability to fluoresce. The resulting Q-type emission bands, like the Q-type absorption bands, are substantially red-shifted (by >100 nm) compared to typical porphyrins.<sup>25,26</sup> This combination of spectral and redox features made texaphyrins attractive for study in the context of certain biomedical applications.

Some of the first biological tests with compound **1** involved MRI studies. It was found to be easily visualized by this modality and to enhance the contrast of MRI images substantially. These attractive findings were ascribed to the centrally coordinated paramagnetic metal cation gadolinium(III),<sup>27</sup> which serves to enhance the effective spin–lattice relaxation ( $T_1$ ). On the basis of the initial MRI analyses, **1** was found to localize well in tumors. No appreciable localization in adjacent normal tissue was observed.<sup>28</sup> Additional MRI studies conducted by Viala et al. provided further evidence for the proposed tumor selectivity of **1**.<sup>29</sup> The ratio of **1** in tumor cells to that in surrounding normal cells was reported to be up to 9:1.<sup>30</sup> As inferred from MRI images, this ratio increases to 50:1 in the case of metastatic brain tumors.<sup>31</sup> The uptake in target lesions was higher after 10 daily injections than after the first dose. This finding was interpreted in terms of an ability to accumulate and persist in brain metastases. In clinical tests, the response to treatment at successive MRI examinations could be evaluated as well because either gadolinium texaphyrin or the gadolinium(III) cation, originally contained in its core, was found to remain in tumorous lesions for several months. This could be of practical benefit in the context of a treatment regimen.<sup>29</sup>

Initially, compound **1** was developed by Pharmacyclics, Inc., as an experimental drug that was considered attractive for use in the treatment of patients suffering from non-small-cell lung cancer (NSCLC) with brain metastases. However, after a phase III study revealed tantalizing signs of efficacy, but without

meeting the prenegotiated statistical end points, **1** failed to obtain FDA approval in December 2007.<sup>32</sup> Although limited clinical studies of **1** are ongoing, this failure has served as an incentive to define new research goals for texaphyrins and to explore other cancer-related opportunities for this class of compounds. The following summaries are designed to provide synopses of three projects developed as a result of these refocusing efforts.

**Bismuth- and Lead-Coordinated Texaphyrins.** One area wherein texaphyrins could see further biomedical application involves their use in supporting complexes of main-group elements. In porphyrin chemistry, complexes with post-transition elements, such as gallium, indium, thallium, lead, and bismuth, are rare compared to those of the transition elements.<sup>33</sup> Yet the chemistry of bismuth has become of increasing interest because its <sup>212</sup>Bi and <sup>213</sup>Bi isotopes show promise for use as  $\alpha$ -emitters in radiotherapy.<sup>34,35</sup> Because of the high linear energy-transfer radiation produced (100 keV  $\mu\text{m}^{-1}$ ), these isotopes demonstrate a strong anticancer cell effect under hypoxic conditions.<sup>36</sup> This ultimately leads to double-stranded DNA breaks at levels that preclude efficient cell repair and survival. However, the short half-life of these two isotopes (60.55 and 45.65 min for <sup>212</sup>Bi and <sup>213</sup>Bi, respectively) and the difficulties of administering salts in a biocompatible, disease-specific manner provide an incentive to develop complexing agents that can coordinate the bismuth(III) cation quickly and would then impart a degree of tumor-specific targeting.

Also attractive is the concept of an in situ generator for either <sup>212</sup>Bi or <sup>213</sup>Bi. One approach would involve the initial complexation of lead.<sup>37</sup> One particular lead isotope, <sup>212</sup>Pb, has a half-life of 10.64 h and produces <sup>212</sup>Bi as its primary decay product along with a  $\beta$  particle. Thus, if this precursor isotope (<sup>212</sup>Pb) could be complexed readily, it would allow for the effective production of the corresponding <sup>212</sup>Bi complex.

Finding suitable ligands for bismuth or lead has proved challenging. An ideal ligand would be one that is able to form stable complexes with both bismuth and lead rapidly and to do so under mild conditions. Complexes of bismuth and lead that possess inherent tumor selectivity would be further advantageous because they would allow the radioactive species in question, namely, <sup>212</sup>Bi, <sup>213</sup>Bi, or <sup>212</sup>Pb, to be delivered selectively to cancerous tissues. This led us to suggest that texaphyrin would be an ideal ligand for these metals. As noted above, texaphyrins have been shown to localize to, or be retained selectively in, rapidly growing tissues, including cancerous lesions; they are thus attractive as carriers for these radioisotopes.<sup>38</sup>

As demonstrated recently, texaphyrin is indeed able to complex the bismuth(III) and lead(II) cations rapidly [reaction in methanol at 75 °C complete after 34 min in the case of bismuth(III) and 98 min in the case of lead(II)].<sup>39</sup> Specifically, spectroscopic and mass spectrometric evidence was put forward to support formation of the first lead(II) texaphyrin complexes **33** and **35** (cf. Figure 5). Similar methods were used to confirm formation of the first discrete binuclear  $\mu$ -oxobismuth(III) macrocyclic complex **34**, a system that was further characterized via single-crystal X-ray diffraction analysis.<sup>39</sup>

These newly prepared lead(II) and bismuth(III) texaphyrin complexes proved chemically stable despite the  $\mu$ -oxo bond present in the latter complex. This allowed the water-soluble derivatives to be studied in vitro using the A2780 ovarian cancer cell line. On this basis, it was concluded that the lead(II)

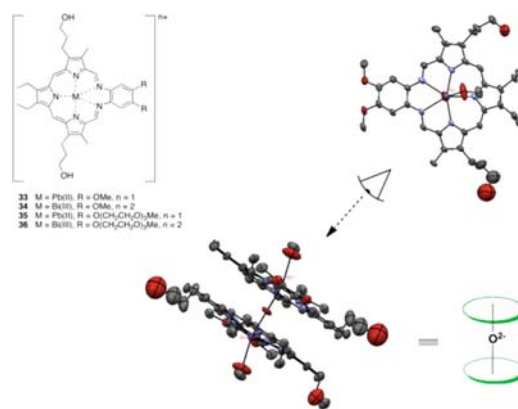


**Figure 5.** Lead and bismuth texaphyrins **33–36** and views of the single-crystal X-ray structure of complex **34**.

texaphyrin **35** and the bismuth(III) texaphyrin **36** gave half-maximal inhibitory concentration ( $\text{IC}_{50}$ ) values of 2.9 and 2.2  $\mu\text{M}$ , respectively. This represents a 2–3-fold increase in cytotoxicity relative to **1** (6.3  $\mu\text{M}$ ).<sup>40</sup> On the basis of these findings and considering the tumor selectivity properties of texaphyrins, we suggest that the texaphyrins could emerge as useful complexants for <sup>212</sup>Bi, <sup>213</sup>Bi, or <sup>212</sup>Pb and, as such, warrant further study as candidates for radiotherapy.

**Texaphyrin-Functionalized Magnetic Nanoparticles (MNPs).** Achieving high accuracy and precision are the main challenges in a variety of imaging techniques, including MRI. Typical MRI contrast agents are comprised of either paramagnetic materials for  $T_1$ -weighted scans (i.e., to depict differences in the spin–lattice relaxation time of various tissues) or superparamagnetic nanoparticles for  $T_2$ -weighted scans (i.e., to depict differences in the spin–spin relaxation time).<sup>41–44</sup> However, such single-mode contrast agents are far from ideal, particularly when accurate imaging of small biological targets is required.<sup>45,46</sup> One of us (J.C.) put forward a potential solution to this problem via the development of MNPs that can act as dual-mode MRI contrast agents (DMCAs).<sup>47</sup> The so-called “magnetically decoupled” core–shell design of these nanoparticles consists of a  $T_2$  active core (e.g.,  $\text{MnFe}_2\text{O}_4$ ) and a  $T_1$  active material [ $\text{Gd}_2\text{O}(\text{CO}_3)_2$ ] located on the shell.

The initial goal of this project was thus to use gadolinium(III) texaphyrins as the  $T_1$  contrast material in a DMCA system. With this consideration in mind, gadolinium(III) texaphyrin **37**-conjugated magnetic nanoparticle constructs (GdTx-MNP), consisting of a zinc-doped iron oxide  $T_2$  core coated with a layer of silicon dioxide functioning as a separating layer, were prepared. In this case, the final conjugation step results in the formation of constructs where the texaphyrin macrocycles are covalently linked to the surface of the nanoparticles.<sup>48</sup>

The elaborated nanoparticle systems were then tested as DMCAs. While contrast agents used clinically, such as Magnevist<sup>38</sup> and Feridex, display either only bright  $T_1$  or dark  $T_2$  contrast, in an MRI phantom study, GdTx-MNP was found to give rise to intense MRI signals in both modes (cf. Figure 6). Simultaneous bright  $T_1$  and dark  $T_2$  contrast effects are ascribable to the gadolinium texaphyrin ( $T_1$  active material) and magnetic nanoparticle ( $T_2$  active material) portions of the constructs, respectively. In contrast, MRI images associated with the control groups and the commercially available contrast

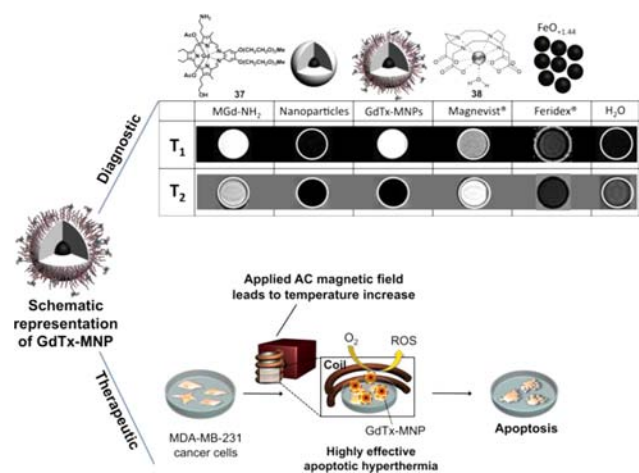


**Figure 6.** DMCA enhancements ( $T_1$  and  $T_2$  modes are shown; note that a bright contrast in the  $T_1$  mode and a dark contrast in the  $T_2$  mode are desired in MRI images of tumorous tissues) and anticancer activity that is ascribed to a combination of sensitization (ROS production) and hyperthermia.<sup>48</sup>

agents Magnevist<sup>38</sup> and Feridex display either only bright  $T_1$  or dark  $T_2$  contrast, but not both.

Additionally, we demonstrated that the GdTx-MNP construct can effectively sensitize cancer cells (here: MDA-MB-231, a breast cancer cell line) in vitro and in vivo, making them highly vulnerable to apoptotic magnetic hyperthermia at low temperatures (Figure 6).<sup>48</sup> This enhancement was ascribed to the ability of the texaphyrins to produce ROS under the conditions of the experiment.

The in vivo studies involved xenograft mouse models. These models were produced by injecting MDA-MB-231 cells into the right hind leg of nude mice in a series of experimental groups ( $n = 3$ ). A dispersion of GdTx-MNPs (75  $\mu\text{g}$ , dispersed in 50  $\mu\text{L}$  normal saline) was directly injected into the tumor tissue (100  $\text{mm}^3$ ). The mouse was then placed in a water-cooled magnetic induction coil (Figure 7a) and an AC magnetic field (500 kHz at 30  $\text{kA m}^{-1}$ ) was applied to maintain a constant temperature at the tumor ( $43 \pm 1$  °C) for 30 min. This hyperthermia treatment was applied once, and the tumor size was monitored for 14 consecutive days. In the mice making up the untreated control group, the average tumor size increased approximately 7-fold by day 14 (Figure 7b,c). However, for the group receiving hyperthermia treatment with GdTx-MNPs, the tumors were absent after 8 days (Figure 7b,c). For comparison, another group of mice was subjected to hyperthermia treatment after administration of unfunctionalized MNPs at an identical dosage. Although the size of the tumors regressed initially, a significant amount of tumor mass remained at day 8 ( $V/V_{\text{initial}} = 0.6$ ), and the tumors started to regrow at day 12.<sup>48</sup>

Until now, attempts to use low-temperature magnetic hyperthermia for cancer therapy have proved challenging because of the development of thermal tolerance. The dramatic reduction in tumor burden seen in vivo and the high degree of efficacy seen in vitro using the texaphyrin-functionalized nanoparticles are ascribed to the sensitization effect arising from ROS production as noted above. The efficient heat generation produced by GdTx-MNPs is also advantageous because lower concentrations of nanoparticles are necessary to achieve the hyperthermia temperature (43 °C). The pathway of cell death involves predominantly apoptosis, a mode of action that is considered beneficial for ultimate clinical use. Given

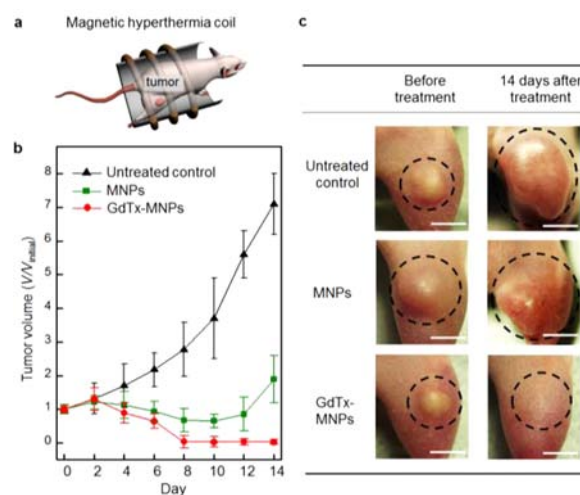


**Figure 7.** In vivo magnetic hyperthermia: (a) Injection of GdTx-MNPs into the right hind leg of nude mice and application of an AC magnetic field for 30 min. (b) Plot of the tumor volume ( $V/V_{\text{initial}}$ ) versus the number of days after treatment. Three different groups were either untreated, treated with unfunctionalized MNPs, or treated with GdTx-MNP hyperthermia. (c) Images of xenografted tumors (MDA-MB-231) on nude mice before treatment (left column) and 14 days after treatment (right column). Note the different outcomes for untreated control and the mice subjected to hyperthermia with MNPs and GdTx-MNPs. Each scale bar indicates 5 mm.<sup>48</sup>

these features, we propose that double effector nanoparticles, such as the texaphyrin-bearing systems produced to date, could emerge as a new approach to achieving apoptotic magnetic hyperthermia.

**Texaphyrin–Platinum Conjugates.** Building on the appreciation that texaphyrins display tumor-selective localization features, our group became intrigued by the possibility that texaphyrins could act as active delivery vehicles for other known cancer therapeutics. We considered this approach for drug delivery to be attractive relative to other potentially competing strategies (i.e., pegylation, liposomal formulation, etc.) in that the carrier (i.e., texaphyrin) itself is well-tolerated and effective at cancer targeting; it also shows some promise as an anticancer agent (vide supra). To test this potential, an effort was made to create conjugates containing platinum(II) centers. The hope was that this would allow certain mechanisms of platinum resistance to be overcome.

While active in several cancer types and included in front-line therapy by oncologists, platinum anticancer agents display acquired resistance in many cancers, which limits their clinical utility. The cause of this resistance is multifactorial and includes both pharmacological mechanisms (e.g., decreased drug uptake, increased GSH, and increased DNA adduct repair) and molecular mechanisms of resistance [e.g., a loss of the tumor suppressor protein 53 (p53) function, an increase in survivin, and an increase in B-cell lymphoma 2].<sup>49–51</sup>

A major incentive for using texaphyrin as a “carrier” involved the challenge of overcoming platinum drug resistance, particularly as applied to ovarian cancer. The FDA-approved platinum drugs cisplatin 39, carboplatin 40, and oxaliplatin 41 (cf. Figure 8) are widely used cancer therapeutic agents.<sup>52–55</sup> Cisplatin and carboplatin, however, are the main agents used in ovarian cancer.<sup>56</sup> The mode of action of platinum-based agents is the formation of platinum–DNA adducts, which, in turn, activate several signal transduction pathways, eventually leading

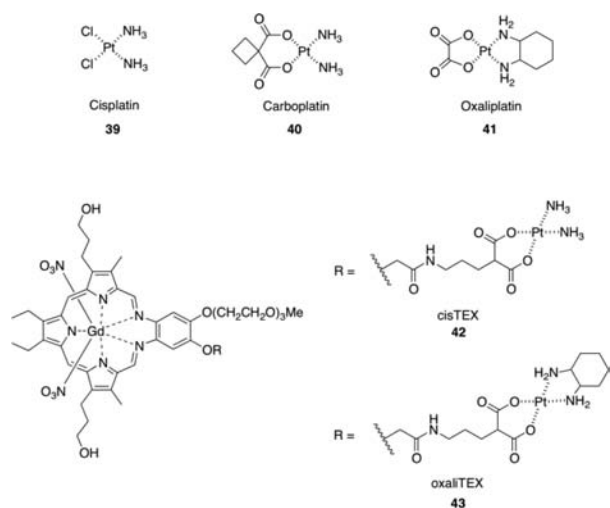


**Figure 8.** FDA-approved platinum drugs and texaphyrin–platinum(II) conjugates **42** and **43**.

to apoptosis. In several cell lines, platinum resistance has become a major factor, recapitulating a key limitation in terms of the clinical use of platinum-based drugs. In the clinic, resistance serves to compound the inherent limitations of the platinum drugs, including systemic (and often dose-limiting) toxicity that reflects, at least in part, a lack of tumor-specific tissue distribution.

We began exploring the hypothesis that the conjugation of platinum to a tumor-localizing texaphyrin would serve to overcome some platinum resistance pathways, such as reduced accumulation and fewer platinum–DNA lesions and thus ultimately reactivate p53-mediated apoptosis via increased accumulation of intracellular platinum. Toward this end, we designed and synthesized a novel texaphyrin platinum conjugate (cisTEX **42**; Figure 8). A pair of ovarian cancer models, consisting of a platinum-sensitive A2780 cell line and its isogenic platinum-resistant 2780CP cell line, were chosen to determine whether this conjugate was effective in overcoming resistance.<sup>40</sup>

Cell proliferation assays were used initially to assess the cytotoxicity and probe antiresistance benefits (Table 1). Conjugate **42** provided cytotoxicity profiles similar to that of carboplatin and other controls in the ovarian A2780 model. In addition, complex **42** provided higher cytotoxicity than compound **1**. However, conjugate **42** provided greater cytotoxicity (i.e., lower IC<sub>50</sub>) than carboplatin against

**Table 1.** IC<sub>50</sub> Values of Platinum Complexes with Cisplatin-Sensitive A2780 Ovarian and Its Isogenic Cisplatin-Resistant Cell Line (2780CP) (Data Are Shown as Mean ± SD)

complex	IC <sub>50</sub> (μM)		resistance factor
	A2780	2780CP	
cisTEX <b>42</b>	1.4 ± 0.3	14.4 ± 1.7	10.3 ± 1.3
carboplatin <b>40</b>	1.6 ± 0.3	26.3 ± 4.1	16.4 ± 5.2 <sup>a</sup>
cisplatin <b>39</b>	0.31 ± 0.06	7.1 ± 0.9	22.9 ± 5.3 <sup>a</sup>
oxaliTEX <b>43</b>	0.55 ± 0.06	0.65 ± 0.09	1.2 ± 0.18
oxaliplatin <b>41</b>	0.15 ± 0.05	0.30 ± 0.05 <sup>a</sup>	2.0 ± 0.29
complex <b>1</b>	6.3 ± 0.6	13.7 ± 0.8	2.2 ± 0.38

<sup>a</sup>*p* < 0.05 by the Student's *t* test versus resistance factor for conjugate **42**.

platinum-resistant 2780CP cells. In terms of the associated resistance factor (reflecting the difference between resistant and sensitive cell lines), conjugate **42** provided the lowest value in its class and proved to be about 32–55% lower relative to cisplatin **39** and carboplatin **40**. This finding was considered indicative of a partial circumvention of cisplatin resistance. It was later determined that the decrease in the resistance factor of conjugate **42** is due to increased intracellular platinum provided by conjugation to texaphyrin (cf. Figure 9).<sup>56</sup>

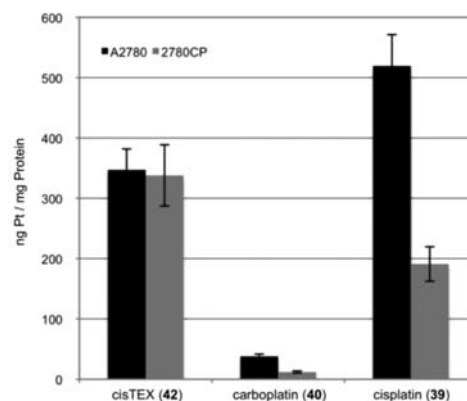


**Figure 9.** Cellular uptake of platinum drugs. Levels of intracellular platinum in A2780 and 2780CP were determined by flameless atomic absorption spectrophotometry (FAAS) after 4 h of incubation with 200 μM of the respective complex (concentrations confirmed by FAAS). *p* < 0.05 by the Student's *t* test for platinum uptake of cisplatin and oxaliplatin in 2780CP vs A2780.

In fact, a 12-fold increase in intracellular platinum from conjugate **42** was detected relative to carboplatin. Additionally, no reduction was seen in the uptake of platinum between the A2780 and 2780CP cell lines with conjugate **42**, whereas a >50% reduction was observed in platinum-based controls carboplatin and cisplatin. This significant increase in intracellular platinum with conjugate **42** resulted in the increased formation of platinum–DNA adducts in both the A2780 and 2780CP cell lines, presumably accounting for the reduced resistance compared to control complexes. However, it was found that while intracellular platinum accumulation was increased and a relatively increased number of platinum–DNA lesions were seen, the type of platinum delivered and the resultant adduct were not capable of reactivating p53 activity in resistance cells. This was evidenced by DNA damage tolerance, with the levels of cisTEX being similar to that of cisplatin in both A2780 and 2780CP.<sup>56</sup>

To address this, we then focused on two major cisplatin-resistance mechanisms, reduced drug uptake and attenuated wild-type p53 function. Specifically, we sought to target these mechanisms via a novel platinum drug design. With this goal in mind, we designed the second generation conjugate **46** (oxaliTEX).<sup>57</sup> The focus on this design reflected a desire to target the tumor suppressor p53 and derived from an appreciation that cisplatin has a greater curative rate in ovarian cancer when p53 is present in its wild-type state than in the mutant form.<sup>50,51</sup>

Paradoxically, about half of advanced ovarian cancers that harbor wild-type p53 are resistant, primarily as a result of failure of upstream DNA damage signaling to stabilize and activate p53. Furthermore, in these resistant cancers, the presence of wild-type p53 can lead to a “gain-of-resistance” phenotype,

where the resistance is greater than those with mutant p53.<sup>50,51</sup> Thus, the loss of function of wild-type p53 is one of the most formidable molecular mechanisms of resistance. However, we have reported that a panel of resistant ovarian tumor models respond to diaminocyclohexyl (DACH)-based platinum drugs through distinctly different DNA damage signaling processes that serve to restore p53 function and cellular apoptotic activity.<sup>58–60</sup> Such a restoration of activity was considered likely to hold in the case of DACH-based oxaliplatin and was specifically confirmed using the resistant 2780CP cell line as detailed below.

To test our hypothesis, we synthesized and studied conjugate oxaliTEX 43 by cell proliferation assays with our ovarian cancer models (Figure 10 and 11, respectively). OxaliTEX 43 ( $IC_{50}$  =

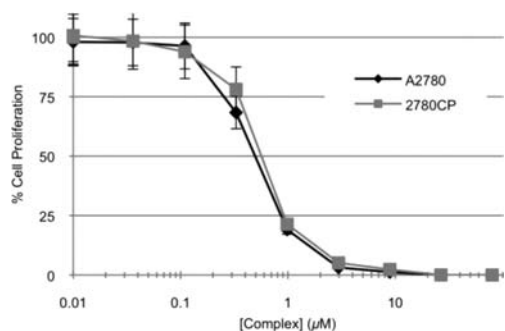


**Figure 10.** Cytotoxicity profiles of oxaliTEX 43 with cisplatin-sensitive A2780 and cisplatin-resistant 2780CP. The complex was made up as a stock solution (for which the platinum concentration was confirmed by FAAS) and serially diluted before addition to cells, which were then incubated for 5 days at 37 °C in 5% CO<sub>2</sub>. Error bars represent the standard deviation.

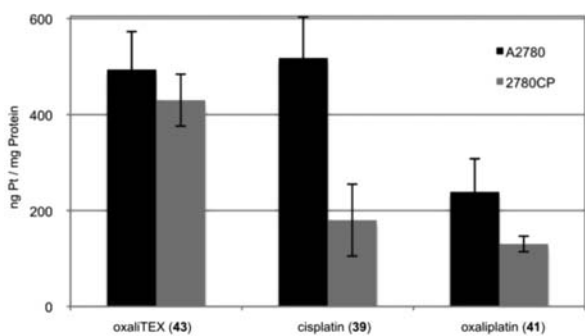


**Figure 11.** Cellular uptake of platinum drugs. Levels of intracellular platinum in A2780 and 2780CP were determined by FAAS after 4 h of incubation with 200 μM of the respective complex (concentrations confirmed by FAAS).  $p < 0.05$  by the Student's  $t$  test for platinum uptake of cisplatin and oxaliplatin in 2780CP vs A2780.

$0.55 \pm 0.06 \mu\text{M}$ ) provided a dose potency in the A2780 cell line that was nearly 3-fold greater than that of cisTEX ( $IC_{50}$  =  $1.63 \pm 0.2 \mu\text{M}$ ). Against 2780CP cells, oxaliTEX 43 and oxaliplatin 41 (both containing DACH) maintained their potent activities, with  $IC_{50}$  values of  $0.65 \pm 0.09$  and  $0.30 \pm 0.05 \mu\text{M}$ , respectively. In contrast, cisTEX and cisplatin provided values that reflect a 11–26-fold lower potency relative to oxaliTEX. It was demonstrated that 2780CP cells were 2-fold cross-resistant to oxaliplatin but were almost devoid of cross-resistance to conjugate 43 (cross-resistance factor, 1.2). This is consistent with essentially complete circumvention of resistance.

That the apparent activation of wild-type p53 is sufficient to overcome multifactorial molecular mechanisms of resistance is intriguing. Normally, wild-type p53 plays a critical role in drug-induced apoptosis. However, this activity becomes compromised when p53 is mutated, which leads to cisplatin/carboplatin resistance and, in the specific case of advanced ovarian cancer for which statistics are available, a 4–5-fold reduction in the 5 year survival rate compared to the wild-type p53 cancer subgroup.<sup>50,51</sup> Advanced cancers other than ovarian cancer (e.g., NSCLC and mesothelioma) that retain wild-type p53 also demonstrate resistance to cisplatin,<sup>51</sup> an observation ascribed to a number of mechanisms, including the critical post-translational modifications of p53 to release p53 from its inhibitory interaction with mouse double minute 2 homologue.<sup>61,62</sup> On the basis of reports from molecularly engineered mouse models,<sup>63</sup> it appears that activation of wild-type p53 and associated induction of apoptosis are dominant results of DNA damage and are sufficient to override the potential negative influence of other molecular defects that may coexist in multifactorial resistant tumor cells.

The 2780CP tumor cells used as a model for platinum resistance in ovarian cancer have been characterized as having a multifactorial cisplatin-resistance phenotype.<sup>58</sup> It was demonstrated that oxaliTEX restored platinum sensitivity, as evidenced by induction of apoptosis (studied via flow cytometry) and upregulation of p53, phosphorylated p53, and p21 (studied via Western Blot analysis). It was also demonstrated from apoptotic investigations using Annexin V as a biomarker that the texaphyrin control, 1, is devoid of antiproliferative effects at concentrations that were equivalent to those employed in the studies of oxaliTEX 43.

Although circumventing molecular mechanisms of resistance can be ascribed to the design of the conjugate, the potency of oxaliTEX still relies heavily on achieving effective platinum concentrations within tumor cells. Our studies served to demonstrate that oxaliTEX (cf. Figure 11) was capable of delivering the DACH-Pt payload at similar levels in both sensitive and resistant tumor cells, a process similarly observed in cisTEX (cf. Figure 9). The similar delivery of platinum is likely due to the inherent features of the expanded porphyrin, texaphyrin, an essentially flat aromatic core that has been shown to localize selectively within tumors.<sup>64,65</sup> That the effective delivery of platinum is due to the conjugating texaphyrin carrier and not the DACH-Pt moiety can be inferred from the knowledge that uptake and DNA adduct formation data for oxaliTEX (conjugate 43) mirror those reported by us for cisTEX (conjugate 42), which has an alternate diamine–platinum coordination environment.<sup>57</sup>

## CONCLUSIONS

The results obtained to date provide support for our suggestion that texaphyrins could have a role to play in a variety of biomedical areas. These include, but are not limited to, use as anticancer treatments, isotope delivery vehicles, MRI contrast agents, and site-localizing carriers. Their unique mode of action, involving electron capture from ascorbate and other reducing species, as well as the commensurate production of ROS, makes texaphyrins attractive scaffolds for further biological studies. Also attractive is the chemical versatility of the texaphyrins, which offer several sites for chemical modification and functionalization. It is hoped that this review, covering recent advances in the chemistry, synthesis, and biological testing of new texaphyrin derivatives, will inspire additional efforts to

develop more fully the biomedical potential of this class of expanded porphyrins.

## AUTHOR INFORMATION

### Corresponding Author

\*E-mail: sessler@cm.utexas.edu.

### Author Contributions

All authors contributed either to the writing of this article or to the development of the original reports upon which it is based. All authors have given approval to the final version of the manuscript.

### Notes

The authors declare no competing financial interest.

## ACKNOWLEDGMENTS

This work was supported by the Cancer Prevention and Research Institute of Texas (CPRIT; Grant RP 120393 to J.L.S.), the U.S. National Cancer Institute (Grant CA-68682 to J.L.S. and Grants CA-127263 and CA-160687 to Z.H.S.), and the Robert A. Welch Foundation (Grant F-1018 to J.L.S.). Collaborative grant support from UT Austin TI-3D (Robert A. Welch Foundation Grant H-F-0032) and UT MD Anderson Cancer Center CCD (Grant 1003020-2100) is also acknowledged. J.F.A. was supported by a postdoctoral fellowship (Grant PF-11-015-01-CDD) from the American Cancer Society. The work on texaphyrin-functionalized nanoparticles was supported by grants from the Creative Research Initiative (Grant 2010-0018286 to J.C.). This research was further supported by a World Class University program funded by the Ministry of Education, Science and Technology through the National Research Foundation of Korea (Grant R32-10217).

## REFERENCES

- (1) Otto, S. E. *Pocket guide to oncology nursing*; Mosby-Year Book, Inc.: St. Louis, MO, 1995.
- (2) Gates, R. A.; Fink, R. M. *Oncology nursing secrets*; Hanley and Belfus, Inc.: Philadelphia, PA, 1997.
- (3) Mehta, M. P.; Shapiro, W. R.; Phan, S. C.; Gervais, R.; Carrie, C.; Chabot, P.; Patchell, R. A.; Glantz, M. J.; Recht, L.; Langer, C.; Sur, R. K.; Roa, W. H.; Mahe, M. A.; Fortin, A.; Nieder, C.; Meyers, C. A.; Smith, J. A.; Miller, R. A.; Renschler, M. F. *Int. J. Radiat. Oncol. Biol. Phys.* **2009**, *73*, 1069–1076.
- (4) Sessler, J. L.; Hemmi, G. W.; Mody, T. D.; Murai, T.; Burrell, A. *Acc. Chem. Res.* **1994**, *27*, 43–50.
- (5) Mody, T. D.; Sessler, J. L. In *Supramolecular Materials and Technologies*; Reinhoudt, D. N., Ed.; Wiley: Chichester, U.K., 1999; Vol. 4, pp 245–299.
- (6) Mody, T. D.; Fu, L.; Sessler, J. L. In *Progress in Inorganic Chemistry*; Karlin, K. J., Ed.; Wiley: Chichester, U.K., 2001; Vol. 49, p 551.
- (7) Sessler, J. L.; Mody, T. D.; Hemmi, G. W.; Lynch, V. *Inorg. Chem.* **1993**, *32*, 3175–3187.
- (8) Sessler, J. L.; Tvermoes, N. A.; Guldi, D. M.; Mody, T. D. *Phys. Chem.* **1999**, *103*, 787–794.
- (9) Patel, H.; Mick, R.; Finlay, J.; Zhu, T. C.; Rickter, E.; Cengel, K. A.; Malkowicz, S. B.; Hahn, S. M.; Busch, T. M. *Clin. Cancer Res.* **2008**, *14*, 4869–4876.
- (10) Sessler, J. L.; Tvermoes, N. A.; Guldi, D. M.; Hug, G. L.; Mody, T. D.; Magda, D. *J. Phys. Chem. B* **2001**, *105*, 1452–1457.
- (11) Jasat, A.; Dolphin, D. *Chem. Rev.* **1997**, *97*, 2267–2340.
- (12) Sessler, J. L.; Murai, T.; Lynch, V.; Cyr, M. *J. Am. Chem. Soc.* **1988**, *110*, 5586–5588.
- (13) Sessler, J. L.; Murai, T.; Lynch, V. *Inorg. Chem.* **1989**, *28*, 1333–1341.

- (14) Sessler, J. L.; Johnson, M. R.; Lynch, V.; Murai, T. *J. Coord. Chem.* **1988**, *18*, 99–104.
- (15) Cotton, F. A.; Wilkinson, G. *Advanced Inorganic Chemistry*, 4th ed.; John Wiley: New York, 1980; pp 589 and 982.
- (16) Maiya, B. G.; Mallouk, T. E.; Hemmi, G. W.; Sessler, J. L. *Inorg. Chem.* **1990**, *29*, 3738–3745.
- (17) Sessler, J. L.; Mody, T. D.; Ramasamy, R.; Sherry, A. D. *New J. Chem.* **1992**, *16*, 541–544.
- (18) Hannah, S.; Lynch, V.; Guldi, D. M.; Gerasimchuk, N.; MacDonald, C. L. B.; Magda, D.; Sessler, J. L. *J. Am. Chem. Soc.* **2002**, *124*, 8416.
- (19) Guldi, D. M.; Mody, T. D.; Gerasimchuk, N. N.; Magda, D.; Sessler, J. L. *J. Am. Chem. Soc.* **2000**, *122*, 8289–8298.
- (20) Acholla, F. V.; Mertes, K. B. *Tetrahedron Lett.* **1984**, *25*, 3269–3270.
- (21) Acholla, F. V.; Takusagawa, F.; Mertes, K. B. *J. Am. Chem. Soc.* **1985**, *107*, 6902–6908.
- (22) Sessler, J. L.; Johnson, M. R.; Lynch, V. *J. Org. Chem.* **1987**, *52*, 4394–4397.
- (23) Sessler, J. L.; Murai, T.; Lynch, V.; Cyr, M. *J. Am. Chem. Soc.* **1988**, *110*, 5586–5588.
- (24) Hemmi, G. W. Ph.D. Dissertation, The University of Texas at Austin, Austin, TX, 1992; pp 41–43.
- (25) Mody, T. D.; Sessler, J. L. *J. Porphyrins Phthalocyanines* **2001**, *5*, 134–142.
- (26) Sessler, J. L.; Dow, W. C.; O'Connor, D.; Harriman, A.; Hemmi, G. W.; Mody, T. D.; Miller, R. A.; Qing, F.; Springs, S.; Woodburn, K. *J. Alloys Compd.* **1997**, *249*, 146–152.
- (27) Young, S. W.; Sidhu, M. K.; Qing, F. *Invest. Radiol.* **1994**, *29*, 330–338.
- (28) Rosenthal, D. I.; Nurenberg, P.; Becerra, C. R.; Frenkel, E. P.; Carbonne, D. P.; Lum, B. L.; Miller, R.; Engel, J.; Young, S.; Miles, D.; Renschler, M. F. *Clin. Cancer Res.* **1999**, *5*, 739–745.
- (29) Viala, J.; Vanel, D.; Meingau, P.; Lartigau, E.; Carde, P.; Renschler, M. F. *Radiology* **1999**, *3*, 755–759.
- (30) Miller, R. A.; Woodburn, K.; Fan, Q.; Renschler, M. F.; Sessler, J. L.; Koutcher, J. A. *Int. J. Radiat. Oncol. Biol. Phys.* **1999**, *45*, 981–989.
- (31) Mehta, M. P.; Shapiro, W. R.; Glantz, M. J.; Patchell, R. A.; Weitzner, M. A.; Meyers, C. A.; Schultz, C. J.; Roa, W. H.; Leibenhout, M.; Ford, J.; Curran, W.; Phan, S.; Smith, J. A.; Miller, R. A.; Renschler, M. F. *J. Clin. Oncol.* **2002**, *20*, 3445–3453.
- (32) Jungbauer, B. Pharmacocyclics' Xcytrin Gets FDA "Not Approvable". For NSCLC Patients with Brain Metastases, The Pink Sheet, Dec 2007.
- (33) (a) Balieu, S.; Bouraiou, A. M.; Carboni, B.; Boitrel, B. *J. Porphyrins Phthalocyanines* **2008**, *12*, 11–18. (b) Halime, Z.; Lachkar, M.; Roisnel, T.; Furet, E.; Halet, J.-F.; Boitrel, B. *Angew. Chem., Int. Ed.* **2007**, *46*, 5120–5124. (c) Halime, Z.; Lachkar, M.; Furet, E.; Halet, J.-F.; Boitrel, B. *Inorg. Chem.* **2006**, *45*, 10661–10669. (d) Lemon, C. M.; Brothers, P. J.; Boitrel, B. *Dalton Trans.* **2011**, *40*, 6591–6609. (e) Michaudet, L.; Richard, P.; Boitrel, B. *Chem. Commun.* **2000**, *17*, 1589–1590. (f) Boitrel, B.; Breede, M.; Brothers, P. J.; Hodgson, M.; Michaudet, L.; Rickard, C. E. F.; Al Salim, N. *Dalton Trans.* **2003**, *9*, 1803–1807.
- (34) Kozak, R. W.; Atcher, R. W.; Gansow, O. A.; Friedman, A. M.; Hines, J. J.; Waldmann, T. A. *Proc. Natl. Acad. Sci. U.S.A.* **1986**, *83*, 474–478.
- (35) Brechbiel, M. W.; Pippin, C. G.; McMurry, T. J.; Milenic, D.; Roselli, M.; Colcher, D.; Gansow, O. A. *J. Chem. Soc., Chem. Commun.* **1991**, 1169–1170.
- (36) Zalutsky, M. R.; Pozzi, O. R. *Quart. J. Nucl. Med. Mol. Imaging* **2004**, *48*, 289–296.
- (37) Kumar, K.; Magerstaedt, M.; Gansow, O. A. *J. Chem. Soc., Chem. Commun.* **1989**, 145–146.
- (38) Sessler, J. L.; Miller, R. A. *Biochem. Pharmacol.* **2000**, *59*, 733–739.
- (39) Preihs, C.; Arambula, J. F.; Lynch, V. M.; Siddik, Z. H.; Sessler, J. L. *Chem. Commun.* **2010**, *46*, 7900–7902.



- (40) Arambula, J. F.; Sessler, J. L.; Fountain, M.; Wei, W.-h.; Magda, D.; Siddik, Z. H. *Dalton Trans.* **2009**, 48, 10834–10840.
- (41) Lauffer, R. E. *Chem. Rev.* **1987**, 87, 901–927.
- (42) Na, H. B.; Song, I. C.; Hyeon, T. *Adv. Mater.* **2009**, 21, 2133–2148.
- (43) Arbab, A. S.; Liu, W.; Frank, J. A. *Expert Rev. Med. Devices* **2006**, 3, 427–439.
- (44) Jun, Y.-w.; Lee, J.-H.; Cheon, J. *Angew. Chem., Int. Ed.* **2008**, 47, 5122–5135.
- (45) Caravan, P. *Chem. Soc. Rev.* **2006**, 35, 512–523.
- (46) Bulte, D. L.; Kraitchman, W. M. *NMR Biomed.* **2004**, 17, 484–499.
- (47) Choi, J.-s.; Lee, J.-H.; Shin, T.-H.; Song, H.-T.; Kim, E. Y.; Cheon, J. *J. Am. Chem. Soc.* **2010**, 132, 11015–11017.
- (48) Yoo, D.; Jeong, H.; Preihs, C.; Choi, J.-S.; Shin, T.-H.; Sessler, J. L.; Cheon, J. *Angew. Chem., Int. Ed.* **2012**, 51, 12482–12485.
- (49) Siddik, Z. H. *Oncogene* **2003**, 22, 7265–7279.
- (50) Siddik, Z. H. In *Drug Resistance in Cancer Cells*; Mehta, K., Siddik, Z. H., Eds.; Springer Science: New York, 2009.
- (51) Martinez-Rivera, M.; Siddik, Z. H. *Biochem. Pharmacol.* **2012**, 83, 1049–1062.
- (52) Bosl, G. J.; Bajorin, D. F.; Sheinfeld, J. In *Cancer of the Testis*; DeVita, V. T. J., Hellman, S., Rosenberg, S. A., Eds.; Lippincott Williams & Wilkins: Philadelphia, PA, 2001.
- (53) Jamieson, E. R.; Lippard, S. J. *Chem. Rev.* **1999**, 99, 2467–2498.
- (54) Kelland, L. R.; Sharp, S. Y.; O'Neill, C. F.; Raynaud, F. I.; Beale, P. J.; Judson, I. R. *J. Inorg. Biochem.* **1999**, 77, 111–115.
- (55) Fuertes, M. A.; Alonso, C.; Pérez, J.-M. *Chem. Rev.* **2003**, 103, 645–662.
- (56) Arambula, J. F.; Sessler, J. L.; Siddik, Z. H. *Bioorg. Med. Chem. Lett.* **2011**, 21, 1701–1705.
- (57) Arambula, J. F.; Sessler, J. L.; Siddik, Z. H. *Med. Chem. Commun.* **2012**, 3, 1275–1281.
- (58) Siddik, Z. H.; Hagopian, G. S.; Thai, G.; Tomisaki, S.; Toyomasu, T.; Khokhar, A. R. *J. Inorg. Biochem.* **1999**, 77, 65–70.
- (59) Hagopian, G. S.; Mills, G. B.; Khokhar, A. R.; Bast, R. C., Jr.; Siddik, Z. H. *Clin. Cancer Res.* **1999**, 5, 655–663.
- (60) He, G.; Kuang, J.; Khokhar, A. R.; Siddik, Z. H. *Gynecol. Oncol.* **2011**, 122, 402–409.
- (61) Sionov, R. V.; Haupt, Y. *Oncogene* **1999**, 18, 6145–6157.
- (62) Shieh, S. Y.; Ikeda, M.; Taya, Y.; Prives, C. *Cell* **1997**, 91, 325–334.
- (63) Kastan, M. B. *Cell* **2007**, 128, 837–840.
- (64) Arambula, J. F.; Preihs, C.; Borthwick, D.; Magda, D.; Sessler, J. L. *Anti-Cancer Agents Med. Chem.* **2011**, 11, 222–232.
- (65) Magda, D.; et al. In *Medicinal Inorganic Chemistry*; Sessler, J. L., Doctrow, S., McMurry, T., Lippard, S. J., Eds.; American Chemical Society Symposium Series 903; Oxford University Press: Oxford, U.K., 2005.